Jurnal
Teknologi

Full Paper

INVESTIGATION OF TORQUE GENERATION CAPABILITY OF MIXED FLOW TURBINE UNDER STEADY STATE CONDITIONS

M. A. S. Izaiddin, A. F. Mustaffa, M. H. Padzillah*

UTM-Centre for Low Carbon Transport in cooperation with Imperial College London, Universiti Teknologi Malaysia, 81310 UTM Johor Bharu, Johor, Malaysia

*Corresponding author
mhasbullah@utm.my

Article history
Received
21 January 2017
Received in revised form
31 May 2017
Accepted
17 August 2017

Graphical abstract

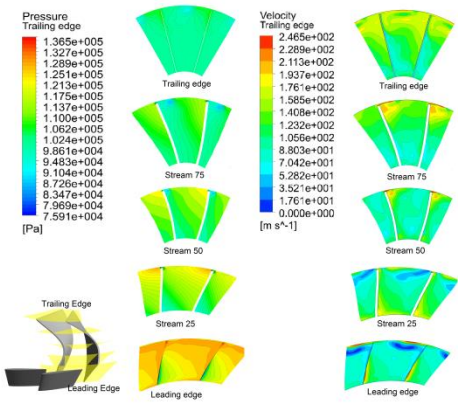

Abstract

A mixed flow turbine is a type of turbine that is used mostly in turbocharger engine for vehicle. The ability of this turbine in obtain maximum efficiency on a wider operating range makes it more favorable compared to axial turbine and radial turbine. In this project, one of the factors affecting turbine performance which is torque has been studied using simulation. The simulation is then being run by varying the mass flow supply to the turbine. In this simulation, torque generation has been identified and plot on the entire blade surface. This torque generation capability is then been compared between 0.25 kg/s, 0.45 kg/s and 0.65 kg/s mass flow. From the simulation, the torque generated is founded to fluctuate along the turbine blade surface. Besides, the torque generated at the leading edge and trailing edge surface are negative. The magnitude of torque generated increases, as the mass flow increased. At the mid span of the blade, torque generated at 0.25 kg/s, 0.45 kg/s and 0.65 kg/s is -3.73 X 10^{-3}Nm, 4.33 X 10^{-3}Nm, and 11.8 X 10^{-3}Nm respectively.

Keywords: Mixed flow turbine, Steady flow, torque, computational fluid dynamics, turbomachinery

1.0 INTRODUCTION

There has been a lot of study in pursuit to obtain the optimum operating condition for the turbine operation either in steady-state condition or pulsating flow condition. In this system, mixed flow turbine is used to extract power from the flowing fluid and turn into mechanical energy liked other normal turbine.

Mixed-flow turbine is a cross over between radial and axial turbines. One advantage of mixed-flow is that it has a lower tendency to generate secondary flows due to its shorter curvature path compared to its radial counterpart [1]. Chen and Baines [2] claimed that mixed flow turbine can function well in low speed range like radial turbine and can have high efficiency in high speed range like axial turbine. It is concluded that the peak efficiency of the turbine occurs at the loading coefficient between 0.9 and 1.0 at flow coefficient in the range 0.2 – 0.3.

Pulsating flow turbochargers due to rapid opening and closure of exhaust valves. Throughout the years, there are numerous papers studying the effect of pulsating flow on turbochargers.

Research on pulsating flow is significant since it represents the actual condition during turbocharger operation. Blair and Wallace [3] found that flow inside radial turbines deviates from quasi-steady assumption when the pulse frequency increase. Acroumanis et. al [4] had studied the performance of mixed flow turbine under pulsating condition. From this study, he conclude that the peak efficiency of mixed flow turbine exists at lower velocity ratio compare to radial turbine which is 0.64 and 0.70 respectively. Karamanis *et al*. [5] found that the inlet

and outlet flow of a mixed flow turbine deviates from the optimum design requirments under pulsating flow. Chiong *et al*. [6]–[9] also used numerical approach to predict the performance of a mixed flow turbine under pulsating flow.

However, due to pulsating flow of the exhaust gas and the complex geometry of mixed flow turbine, there are lot of parameters that periodically changed which can effect the abality of the turbine in extrating energy. At the leading edge of the turbine, the velocity at meridional, tangential and spanwise component are influenced by the pulse wave. This led to fluctuation of flow angle also the incidence angle[10]. Padzillah *et al*. [11] found that the increase of pulsating flow frequency causes a larger variation in flow angle spatial distribution when compared to a lower pulsating frequency. It is also found that the flow angle is more stable during pressure decrement[12]. The variable geometry turbine was then developed to control the vane of the turbine. This will allow the turbine to operate efficiently at wider range of fluid flow. Besides, by this variation of vane, the incidence angle of the flow can be controlled to its optimum range of -20^{o} to -40^{o}[13].

Szymko [14], [15] developed a high-power high-speed eddy current dynamometer for turbine research. This dynamometer is capable to measure torque and significantly improved the experiment ability which this allows the simulation of the engine exhaust pulsation under low temperature become possible. Besides, this dynamometer also allows the turbine to operate in wide loading range of 1.7-62.2 kW at 60000 rpm which was not previously possible.

Padzillah *et al*. [16] has used this dynamometer in his experimental research to provide the validation data for the unsteady state simulation developed by him. In this validation process, the torque recorded for the turbine is fluctuating against time.

The output torque of the turbine are generally used in measuring the performance of the turbine and also validate the simulation developed. Therefore, this work aims to provide detail torque distribution on the turbine surface in a single passage steady state operation condition and its effect against different mass flow rate.

2.0 METHODOLOGY

2.2 Numerical Setup

In order to run the simulation, a 3D model of Rotor A has been developed first. The geometry of this turbine is based to the actual turbine designed by Abidat [8]. Rotor A is chosen as a simulation model since Abidat and many other researchers had used ethis turbine in their actual experiment before. Besides, the availability of experimental results is also important for the turbine configuration validation process. The turbine geometry is first created in the using Turbo grid.

In order to generate a complete single passage mesh, Padzillah *et al*. [18], [19] had developed the same identical rotor using nine profile lines which is done by applying the Bezier Polynomials equation as shown in Figure 1. All of the parameters and constant used in this Bezier Polynomials equation is extracted from Abidat and Padzillah. Hence, the curve of leading edge, trailing edge, hub and shroud are able to be defined smoothly.

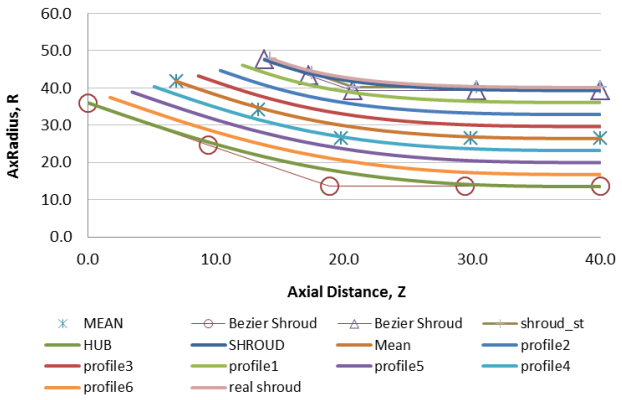

Figure 1 Nine profile lines generated from Bezier Polynomial equation (extracted from Padzillah, [6])

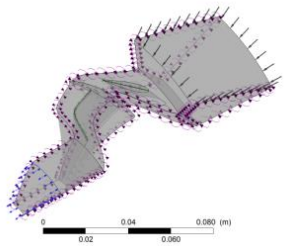

Figure 2 Assembly domain in CFX Pre

In this research, the analysis is solved numerically by using Ansys CFX. Figure 2 shows the assembly domain of turbine rotor in CFX Pre. Then, several boundary conditions have been setup at the vane inlet, turbine outlet and at the wall of the turbine. Vane inlet boundary conditions were referred to the experimental condition at the measurement plane where the temperature was set to be 340 K. The flow regime that entered the turbine was set to be subsonic flow with the angle of 61^{o}. Since the outlet boundary condition, requires the static value, hence the pressure was set to be constant of atmospheric pressure with the approximately of room temperature. The boundary condition of the wall of both vane and rotor were defined to be no slip condition. Mass flow that entered into the turbine was set to be in the range of 0.2 kg/s up to 0.8 kg/s.

2.3 Torque Analysis

Since CFD is able to solve wide-ranging fluid flow in a fast and robust manner, the torque generated is observed from the perspective of the fluid. The force exerted on the blade by the fluid is defined as the multiplication of pressure difference between the blade pressure surface and the blade suction surface with the particular area of that contact surface. Torque on the entire blade is then obtained by multiplying the force with the distance from the center of the turbine as in Equation 1.

$$\sum F = \int dP.dA$$

$$T = Fr \quad (1)$$

This torque analysis is carried out by using CFX Post. As shown in Figure 3, the turbine blade is first divided into three different spanwise plane which then polyline features was used to outline the position of the span. It is possible to plot the pressure distribution along the blade between the pressure surface and the suction surface. In order to get some particular area needed would be the problem in obtaining the resultant force on this polyline. Hence, at each polyline, the turbine had being discretized into 48 small planes along the streamwise location using iso-clip features available in the CFX Post.

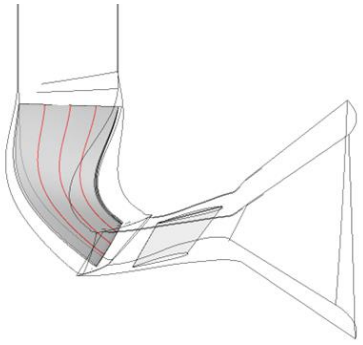

Figure 3 Three polyline used to slice the plan in three spanwise locations

3.0 RESULT AND DISCUSSION

3.1 Validation Process

The result obtained is then validated by comparing the CFD data with the experiment that previously conducted by [5] and [7]. There are four parameters that are being compared which are total to static efficiency, velocity ratio, mass flow parameter, and pressure ratio. All of the parameters used in the validation stage are dimensionless in order to make it compatible with the actual turbine operation.

Velocity ratio is the ratio of the absolute turbine speed over its isentropic absolute speed, C_{is}

$$VR = \frac{U}{C_{is}} \quad (2)$$

Absolute turbine speed and isentropic absolute speed can be calculated by using the formula stated at the equation 3 and 4.

$$U = \pi DN \quad (3)$$

$$C_{is} = \sqrt{2\, c_p\, T_{o1}\left(1 - \left(\frac{P_2}{P_{o1}}\right)^{\frac{\gamma-1}{\gamma}}\right)} \quad (4)$$

Turbine efficiency is defined as the ratio of the turbine actual work over its isentropic work.

$$\eta_{turbine} = \frac{w_{actual}}{w_{isen}} \quad (5)$$

Turbine actual work is defined as the product of the torque of the turbine and the rotational speed of the turbine as in equation 6 while the isentropic work of the turbine is defined as in equation 7.

$$W_a = \tau.\omega \quad (6)$$

$$W_{isen} = \dot{m}\frac{C_{is}^2}{2} \quad (7)$$

As shown in Figure 4(a), the efficiency of the turbine is plotted against the velocity ratio and being compared to the experimental data. The performance of the turbine in this current study shows a good agreement to the turbine used in the experiment. The optimum efficiency of the turbine simulation is slightly lower compared to the experimental data which are 79% and 80% respectively. This is achieved at the velocity ratio of 0.68 where it should generally occur at velocity ratio below than 0.7 since the mixed flow rotor has a positive blade angle[20]. Besides, these values can be accepted as the efficiency and velocity ratio fall in the range of 77% to 80% and 0.57 to 0.68 respectively [4]. The line starts to converge at velocity ratio of 0.75. The small difference in efficiency of simulation parameter may be due to many factors that are not being considered especially in calculating the turbine isentropic efficiency. In this study, the efficiency of the turbine is the factor of only the total temperature and total pressure at the inlet and also the static pressure at the turbine outlet. However, in the actual turbine operation, there are many small factors that contributing in the turbine efficiency which are difficult to be measured.

From Figure 4(b), the turbine mass flow parameter for current study agrees well to the experimental turbine where the lines plotted seem parallel to each other. Besides, this turbine indicates the typical

performance of mixed flow turbine where the mass flow parameter increases as the pressure ratio increase. Hence with these two performance parameters comparison, it can be verified that the current simulation data are valid for further analysis.

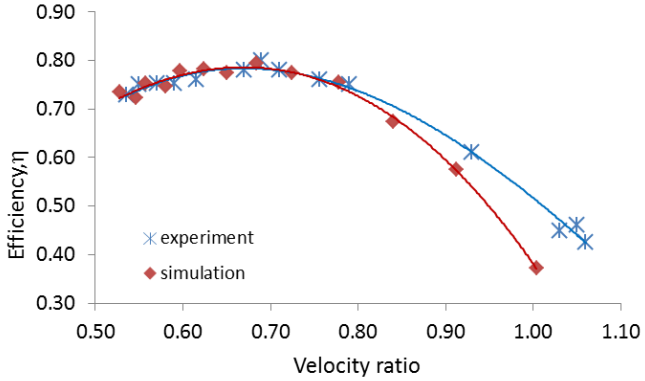

Figure 4(a) Efficiency vs velocity ratio

The mass flow parameter and pressure ratio can be obtain by using equation 8 and 9.

$$MFP = \frac{\dot{m}\sqrt{T_{01}}}{P_{01}} \quad (8)$$

$$PR = \frac{P_{01}}{P_2} \quad (9)$$

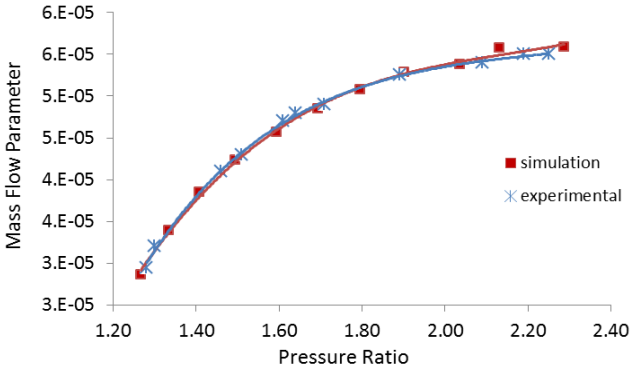

Figure 4(b) Mass flow parameter vs pressure ratio

3.2 Torque Generation Capability

This section presents the torque distribution along the blade surface. The turbine speed is set to be constant at 48,000 rpm and the analysis of torque is focused on the blade at the optimum turbine performance. The torque is being compared at other operating conditions in order to study the behaviour of the torque generated. These three cases are outlined in the Table 1.

Table 1 Three cases for three different operating conditions

Case	Mass flow (kg/s)	Efficiency, η	Velocity ratio
1	0.45	0.79	0.68
2	0.65	0.75	0.58
3	0.25	0.58	0.91

The analysis is done at three different spanwise locations for each case. Figure 4 illustrates the torque behaviour for these three cases. For the optimum turbine performance which is Case 1, Figure 5(a) shows that the torque distributed is fluctuated along the streamwise location of the blade. In each case, the torque generated reduced to zero at 90% to 100% streamwise location which is near to the blade trailing edge. Besides, at the leading edge and the trailing edge of the turbine, negative torque are generated that give disadvantage in terms of turbine rotation.

Moreover, there are significant changes in torque magnitude at these two regions where at the blade leading edge, torque generated is decrease as the flow move towards shroud. However, opposite trend can be observed at the blade trailing edge whereas the flow moves toward shroud, the torque generated become higher. This behavior will be explained further later. Therefore, for the 25% span, torque generated decrease along the streamwise location of the blade while for the 75% span, torque generated increase along the streamwise location of the blade. In contrary to the 50% span, the torque generation can be said to be constant along the blade.

As illustrated in Figure 5(b), torque generated on turbine blade surface in Case 2 is higher than Case 1 at every span location. At this mass flow rate condition, there is no negative torque generated at the leading edge region of turbine blade surface. However, the torque still decreases as the flow move towards the trailing edge and becomes negative starting from 90% streamwise location. In Case 2, behavior of torque generated at 25% span is same as in Case 1 where it decreases as the flow move along the blade. Besides, at 75% span location, behavior of torque generated is also same where it shows opposite trend as in 25% span location. However, for 50% span, behavior of torque generated along the blade surface is different as in Case 1. At this particular condition, torque generated at 50% span seems high at every streamwise location. It recorded highest torque at about 10% streamwise location before decreasing slightly and remain constant above 0.0002 Nm as the flow move along the blade. However, at the middle of the blade, torque generated increase again before becoming negative at the blade trailing edge.

.

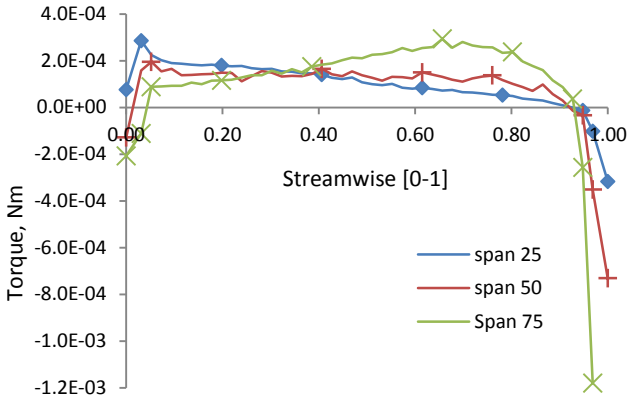

Figure5(a) Torque vs Streamwise location (case 1)

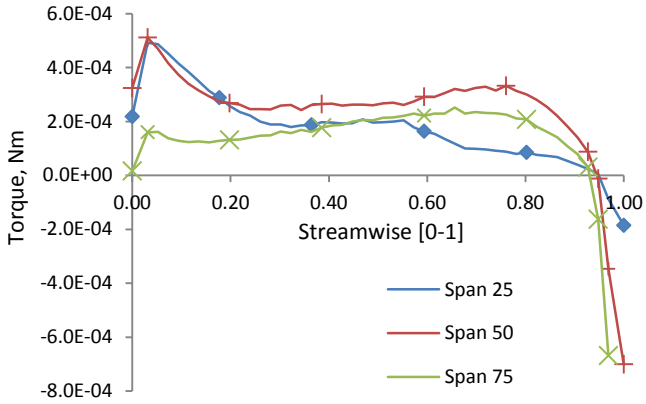

Figure 5(b) Torque vs Streamwise location (case 2)

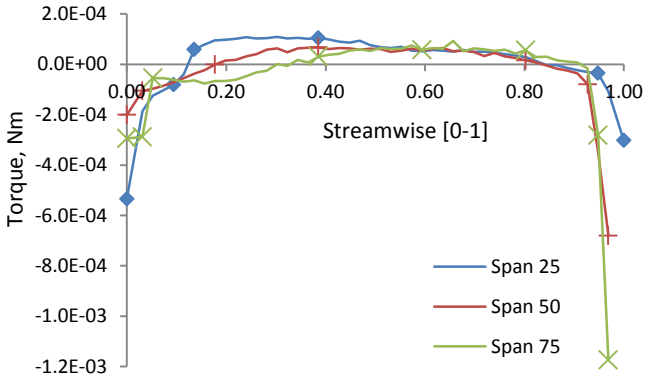

Figure 5(c) Torque vs Streamwise location (case 3)

In Case 3, as shown in Figure 4(c), torque generated at every span is significantly lower compare to other two cases. Slightly changes of torque are only recorded at the early half of the blade. Starting from 50% streamwise location, the torque generated seems similar at every span location.

Therefore, in every cases the behavior of torque generated is identical according to its span location especially for 25% and 75% span; begining from around 10% - 20% streamwise up to 80% to 90% streamwise. Besides, the torque is significantly negative at the trailing edge for every span at all cases. While at the leading edge, torque generated is positive only in Case 2 while the rest are negative.

As discussed earlier, the pressure difference along the blade will theoretically generate force. This force then makes the turbine blade to turn for a certain torque and speed. Hence, pressure difference along the blade surface has been observe and discussed. Case 1 is chosen for this analysis since the optimum efficiency happened at this particular operating condition. Figure 6 shows the pressure and velocity difference along the blade in streamwise plane. Pressure and velocity difference has been plotted in five different planes which are trailing edge, 25% stream, 50% stream, 75% stream and trailing edge of the blade. The pressure across both pressure surface and suction surface are high as the flow enters the blade passage. However, the pressure decrease as the flow moves towards trailing edge. Besides, it can be observed that there is significant high pressure occurrence at the blade shroud. At the leading edge of the blade surface, the pressure at the suction surface is significantly high and form in circular shape especially at the tip of the blade (shroud). This phenomenon is due to large negative incidence angle that occurred at that particular location. According to Chen *et al* [8], one of the factors affecting the blade loading was the incidence angle on the blade. Moreover, negative blade loading at the inlet (especially at the shroud) was due to the large negative incidence angle. Figure 7 illustrate the incidence angle of the blade for this particular condition and location.

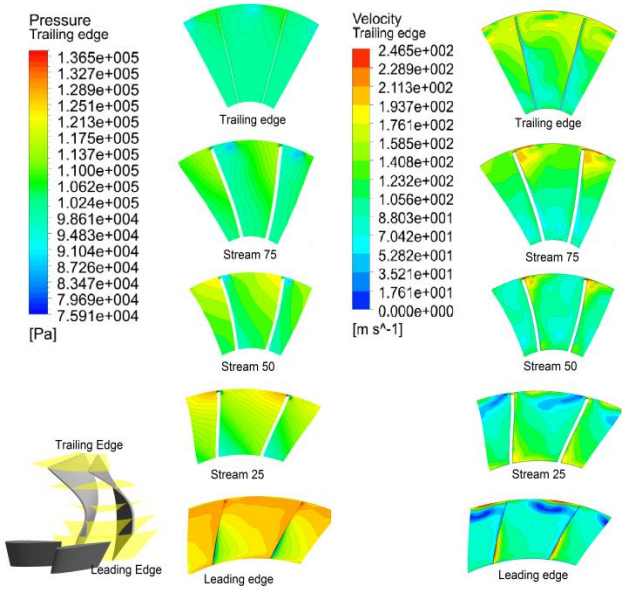

Figure 6 Pressure and velocity contour in streamwise plane

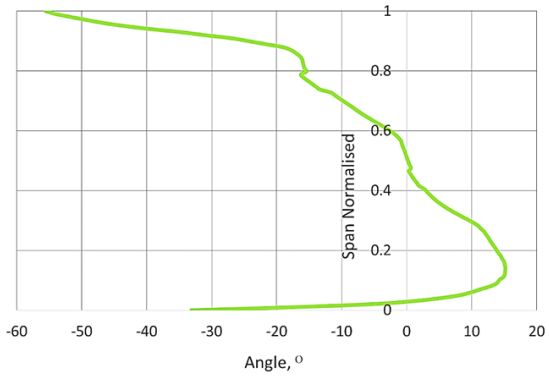

Figure 7 Incidence angle along Span normalized at blade leading edge

From the Figure 7, the incidence angle plotted is found to be largely negative especially when the flow approaches the shroud. Besides, the flow incidence angle cannot be constant at all positions due to the changing radius across the span. Therefore, the flow is not uniform at the entire surface of the turbine. Hence the energy from the flow will not perfectly transfer into mechanical energy on the blade.

However, as the flow move to 25% stream, this high circular pressure turns into low pressure. This circular formation of low pressure move far from the suction surface of the blade until it reaches at the middle of blade to blade direction at the trailing edge of the turbine. This causes the pressure at the pressure surface at the location near to the trailing edge of the blade becomes lower than the suction surface. By referring to the velocity contour, high velocity is recorded to start forming at 25% streamwise location. This formation continues to happen until 75% streamwise location. Karamanis *et al.* [8] mentioned that higher velocities are found at the suction surface compared to the pressure surface is due to the tip clearance flow penetrating into the blade passage along the pressure surface and mixing with the main flow.

At 25% stream to 75% stream, there are no significant changes in pressure contour at the pressure surface of the blade except the normal decreasing trend in magnitude of the pressure. This is due to decreasing of flow area which is caused by the geometry of the turbine. At the suction surface, low pressure is observed especially near the hub. This low pressure then expands to the entire suction surface starting from 50% streamwise to 75% streamwise location. However, the pressure at the suction surface increases as the flow moves towards end of the passage. This can be seen clearly at the shroud of the blade at 100% streamwise or at trailing edge.

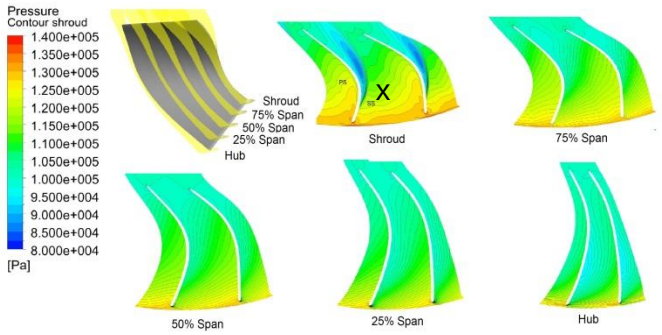

Figure 8 Pressure contour at spanwise plane.

Figure 7 illustrate the different view of the blade where the planes have been sliced in spanwise direction from hub to the shroud. From this view, the pressure generated at the pressure and suction surface are changing as the plane is closer to the shroud. At the turbine hub, the pressure generated at both turbine pressure and the suction surfaces are low as the flow entering the passage. However the pressure is increased as the flow is near to the shroud. Here, the geometry of the turbine is clearly seen to affect the pressure generated by the fluid where the flat surface of the blade will limit the interaction between the fluid and the blade. The flatter the blade is (hub), the lesser pressure acting at the entire blade surface especially at the blade suction surface. However, at the suction surface on the shroud plane, a small core of low pressure seems to form; starting from about 25% stream. This formation of core is may be due to the vortex formation at the suction surface especially at the shroud. The vortex core then moves from the blade suction surface towards the exit of the blade passage.

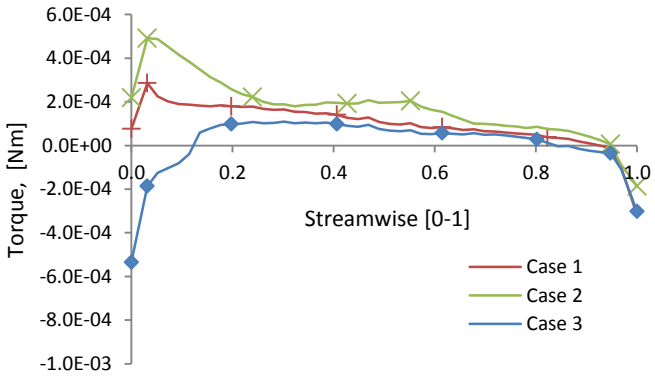

(a) Comparison of torque at 25% spanwise location

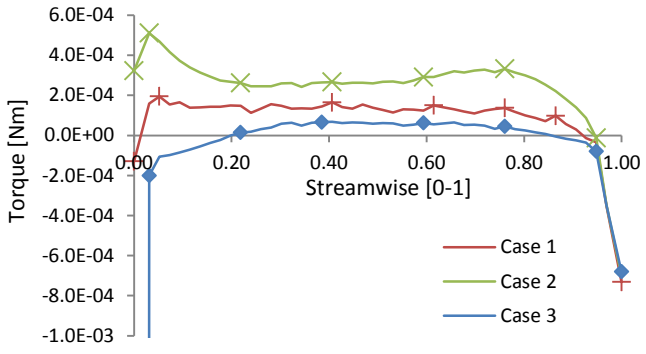

(b) Comparison of torque at 50% spanwise location

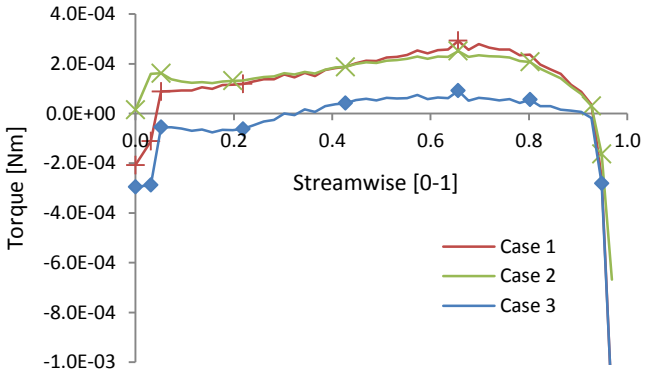

(c) Comparison of torque at 75% spanwise location

Figure 9 Comparison of torque generated at span wise location (a) 25%, (b) 50% and (c) 75%.

The identified torque is then being compared between three cases at the same spanwise location to observe the different and the effect of the mass flow towards the torque generation. Figure 9(a), (b) and (c) illustrate the comparison of torque at 25% spanwise, 50% spanwise and 75% spanwise respectively. From Figure 9, the trend of the torque generated for different mass flow can be said to be identical along the blade surface for Case 1 and Case 2. Case 3 gives a very low torque at 25% span and 50% span. A different trend of torque is generated especially in the region of 20% streamwise location.

Torque generated for Case 3 is also weak where initially, torque generated is negative up to about 10%, 20%, and 30% stream at 25% , 50% and 75% span respectively. Therefore, mass flow of 0.25 kg/s would capable to generate a very low torque especially at the blade shroud. Besides that, the torque would be generated more as the mass flow of the system is high.

4.0 CONCLUSION

This project presents the torque generation capability of mixed flow turbine under steady state condition.

From this project, torque generated has been plot along the streamwise location of the blade surface. The torque generated are found to be fluctuating across the entire blade surface. Besides, torques generated at the trailing edge of all spanwise directions and at different mass flow is recorded to be largely negative. The change of incidence angle especially at the shroud of turbine leading edge also cause the torque generated at the leading edge to be negative. At around the middle of the blade, the change in radius and turbine geometry contribute to different flow speed at the entire blade surface. Besides, the formation of vortex also affects the torque generation where the pressure at this region are lower compare to the other. Hence this will differentiate the torque capability of the blade at different span location.

At different operating condition, torque generated is affected by the mass flow of the turbine passage. Higher mass flow would generate bigger torque on the turbine blade. Unfortunately, torque generated along the blade is not constant. Hence the torque generated by a certain span of the turbine surface would be affected.

Acknowledgement

The author would like to acknowledge Ministry of Higher Education Malaysia and Universiti Teknologi Malaysia FRGS research grant R.J130000.7824.4F833 for their financial support.

References

[1] S. Rajoo and R. Martinez-Botas. 2008. Mixed Flow Turbine Research: A Review. *ASME J. Turbomach.* 130: 12.
[2] H. C. and N. C. Baines. 1994. The Aerodynamic Loading of Radial and Mixed-flow Turbines. 36(1): 63-79.
[3] F. J. Wallace and G. P. Blair. 1965. The Pulsating Flow Performance of Inward Radial-Flow Turbine. *Proc ASME Turbo Expo No. 65-GTP-21*. 1-19.
[4] C. Arcoumanis, I. Hakeem, L. Khezzar, R. F. Martinez-Botas, and N. C. Baines. 1995. Performance of a Mixed Flow Turbocharger Turbine Under Pulsating Flow Conditions. *ASME Pap.* No. 95-GT-210.
[5] N. Karamanis, R. F. Martinez-Botas, and C. C. Su. 2001. Mixed Flow Turbines: Inlet and Exit Flow Under Steady and Pulsating Conditions. *J. Turbomach.* 123(2): 359.
[6] M. S. Chiong, M. H. Padzillah, S. Rajoo, A. Romagnoli, A. W. Costall, and R. F. Martinez-Botas. 2015. Comparison of Experimental, 3D and 1D Model for a Mixed-flow Turbine Under Pulsating Flow Conditions. 77(8): 61-68.
[7] M. S. Chiong, S. Rajoo, R. F. Martinez-Botas, and A. Costall, 2011, Engine Turbocharger Performance Prediction: One-Dimensional Modeling of a Twin Entry Turbine. *Energy Convers. Manag.* 57: 68-78.
[8] M. S. Chiong, S. Rajoo, A. Romagnoli, and R. F. Martinez-Botas. 2012. Single Entry Mixed Flow Turbine Performance Prediction with 1-D Gas Dynamic Code Coupled with

Mean Line Model. *Int. J. Gas Turbine, Propuls. Power Syst.* 4(2): 8-16.
[9] M. S. Chiong, S. Rajoo, A. Romagnoli, A. W. Costall, and R. F. Martinez-Botas. 2015. Non-adiabatic Pressure Loss Boundary Condition for Modelling Turbocharger Turbine Pulsating Flow. *Energy Convers. Manag.* 93.
[10] D. Palfreyman and R. F. Martinez-Botas. 2004. The Pulsating Flow Field in a Mixed Flow Turbocharger Turbine: AN Experimental and Computational Study. *Proceedings of the ASME Turbo Expo 2004*. 5 A: 697-708.
[11] M. H. Padzillah, S. Rajoo, and R. F. Martinez-Botas. 2014. Influence of Speed and Frequency Towards the Automotive Turbocharger Turbine Performance Under Pulsating Flow Conditions. *Energy Convers. Manag.* 80: 416-428.
[12] M. H. Padzillah, S. Rajoo, M. Yang, and R. F. Martinez-Botas, Jul. 2015. Influence of Pulsating Flow Frequencies Towards the Flow Angle Distributions of an Automotive Turbocharger Mixed-Flow Turbine. *Energy Convers. Manag.* 98: 449-462.
[13] S. Rajoo. 2007. Steady and Pulsating Performance of a Variable Geometry Mixed Flow Turbocharger Turbine. Imperial College of Science. Technology and Medicine.
[14] S. Szymko, R. F. Martinez-Botas, and K. R. Pullen. 2005. Experimental Evaluation of Turbocharger Turbine Performance Under Pulsating Flow Conditions. *Turbo Expo 2005, Parts A and B*. 6 PART B: 1447-1457.
[15] S. Szymko, N. R. McGlashan, R. Martinez-Botas, and K. R. Pullen. 2007. The Development of a Dynamometer for Torque Measurement of Automotive Turbocharger Turbines. *Proc. Inst. Mech. Eng. Part D J. Automob. Eng.* 221(2): 225-239.
[16] M. H. Padzillah. 2014. Experimental and Numerical Investigation of an Automotive Mixed Flow Turbocharger Turbine under Pulsating Flow Conditions. PHD Thesis. March.
[17] M. Abidat. 1991. Design and Testing of a Highly Loaded Mixed Flow Turbine. Imperial College of Science. Technology and Medicine, University of London.
[18] M. H. Padzillah, S. Rajoo, and R. F. Martinez-Botas. 2016. Comparison of Flow Field Between Steady and Unsteady Flow of an Automotive Mixed Flow Turbocharger Turbine. *J. Teknol.* 78(8-4).
[19] M. H. Padzillah, S. Rajoo, and R. F. Martinez-Botas. 2016. Pressure Distribution on the Blade Surface of an Automotive Mixed Flow Turbocharger Turbine Under Pulsating Flow Conditions. *J. Teknol.* 78(8-4).
[20] N. Karamanis. 2002. Mixed-flow Turbines for Automotive Turbochargers: Steady and Unsteady Performance. 3(3).